Origin of early Cretaceous calc-alkaline lamprophyres from the Sulu orogen in eastern China: implications for enrichment processes beneath continental collisional belt

Feng Guo[a,*], Weiming Fan[a], Yuejun Wang[a], Ming Zhang[b]

[a]Key Laboratory of Marginal Sea Geology, Guangzhou Institute of Geochemistry and South China Sea Institute of Oceanology, Chinese Academy of Sciences, Wushan, Guangzhou, Guangdong 510640, PR China
[b]ARC National Key Center for Geochemical Evolution and Metallogeny of Continents (GEMOC), Department of Earth and Planetary Sciences, Macquarie University, NSW 2109, Australia

Abstract

K–Ar dating, major- and trace-element and Sr–Nd isotopic analyses were carried out for early Cretaceous (122–127 Ma) lamprophyres from the Sulu orogen in eastern China. The results show strong fractionation in rare-earth elements with (LREE) >100 times chondrite, but HREE <10 times chondrite, indicating the presence of residual garnet in the melting source. These rocks are characterized by significant LILE and LREE enrichment but Nb and Ta depletion with moderate Zr/Hf (39.8–50.8 with regard to 36 for primitive mantle) and Nb/Ta (17.8–23.0, compared with 17.5 for primitive mantle) fractionations, probably as a consequence of carbonate- and rutile-rich melt metasomatism induced by dehydration and/or melting of subducted continental slab at mantle depths. Age-correlated Sr–Nd isotope ratios show moderate ranges of $^{87}Sr/^{86}Sr(i)$ from 0.70787 to 0.70934 and -17.2 to -11.6 of $\varepsilon_{Nd}(t)$. The lamprophyres from the Sulu orogen were derived from decompression melting of such a metasomatized lithospheric mantle that was mainly composed of phlogophite garnet peridotites and experienced crystal fractionation of a mineral assemblage of olivine + clinopyroxene ± plagioclase en route to the surface. Such geochemical and isotopic signatures are also prevalent in the contemporaneous basaltic lavas in the Dabie–Sulu belt, suggesting predominant enrichment processes by carbonate- and rutile-rich metasomatic assemblage beneath the continental collisional belt.
© 2004 Elsevier B.V. All rights reserved.

Keywords: Geochemistry; Lamprophyres; Early Cretaceous; Mantle metasomatism; Continental subduction; The Sulu orogen

1. Introduction

The trace-element signatures of relative enrichment of light rare-earth elements (LREE) and large ion lithophile elements (LILE) to high-field-strength elements (HFSE) (i.e., high LREE/HFSE and LILE/HFSE ratios) in magmas from arcs and orogenic belts are widely accepted as a consequence of enrichment processes induced by dehydration of subducted slabs (e.g., Arculus, 1994; Hunter and Blake, 1995; Turner et al., 1996; Foley et al., 2000; Tiepolo et al., 2000, 2001). Under an oceanic continental subdirection

* Corresponding author. Tel.: +86-20-85290280; fax: +86-20-85290130.

E-mail address: guofengt@263.net (F. Guo).

system, such features are either ascribed to residual rutile and other titanate minerals that contain the HFSE during melting process or preferential enrichment of other incompatible elements to HFSE by slab-derived fluids in the source (e.g., Foley et al., 2000). In the course of subduction of continental lithosphere, however, the nature of enrichment processes that would explain the strong LILE and LREE enrichment relative to HFSE has been rarely discussed. Previous studies considered such features as results of source mixing/contamination or interaction between subducted slab and upper mantle (e.g., Amelin et al., 1996; Jahn et al., 1999; Fan et al., 2001). It is therefore important for further understanding the mantle enrichment processes beneath continental collisional belts with aims to investigate the role of mantle–crust interaction, recycling of subducted continental lithosphere and origins of orogenic magmas.

The Dabie–Sulu high-pressure (HP) to ultrahigh-pressure (UHP) metamorphic belt is widely accepted as the Triassic collisional belt between the North China and Yangtze Blocks (e.g., Li et al., 1999; Ye et al., 1996, 2000; Cong, 1996; Zheng et al., 2002; Jahn et al., 1996). The preservation of HP-UHP minerals such as coesites and diamond inclusions suggest that the continental crust had been subducted to mantle depths and even >200 km (e.g., Xu et al., 1992; Jahn et al., 1996; Li et al., 1999; Ye et al., 1996, 2000). This provides a rare opportunity for unraveling the enrichment processes related to the subduction of continental lithosphere. Due to the paucity of mafic magmatism from ca. 240 to 130 Ma, the fingerprints of metasomatized mantle caused by continental subduction were probably documented in post-orogenic magmas. Fan et al. (2001) considered the early Cretaceous post-orogenic melts along the Sulu orogen to be a result of crust–mantle interaction, and Jahn et al. (1999) suggested that the enriched mantle beneath the northern Dabie orogen was formed through source mixing between the Yangtze middle–lower continental crust and a depleted mantle. Lamprophyres are commonly considered as small-degree melts of LILE- and LREE-enriched mantle sources (e.g., Rock, 1987; Müller and Groves, 1995), so their origin is closely related to the enrichment process during lithospheric evolution. Here, we present K–Ar dating, major-, trace-element and Sr–

Nd isotope data for early Cretaceous lamprophyres from the Sulu orogen, eastern China. These rocks exhibit strong LILE and LREE enrichment relative to HFSE, moderate Zr/Hf and Nb/Ta fractionations as well as highly enriched Sr–Nd isotopic signatures. Such trace-element and isotopic features were inherited from LILE- and LREE-enriched mantle sources that experienced strong metasomatism by a carbonate- and rutile-rich assemblage in response to dehydration melting of the subducted continental slab at high pressures.

2. Geological backgrounds

The Sulu orogen is widely accepted as the eastern extent of the Triassic Qinling–Dabie collisional belt, where the HP-UHP rocks are widely distributed, such as at Rizhao, Qingdao and Weihai (Ye et al., 1996; Cong, 1996; Jahn et al., 1996; Zheng et al., 2003). Along the ENE-trending Wulian–Qingdao–Rongcheng fault, different metamorphic terranes occur. In the north are a late Archean to early Proterozoic terrane of North China Block affinities and the Mesozoic Laiyang basin (e.g., Cao et al., 1990; Zhai et al., 2000; Fan et al., 2001), whereas Proterozoic Jiaonan and Fenzishan Groups with Triassic interbedded UHP rocks occur in south (e.g., Ye et al., 1996; Cong, 1996; Jahn et al., 1996). The occurrence of HP-UHP rocks and voluminous granitoid plutons and associated large-scale gold mineralization make it an important region for studying the orogenic processes of continental subduction, the role of crust–mantle interaction and origins of gold deposits (e.g., Jahn et al., 1996; Ye et al., 2000; Fan et al., 2001; Wang et al., 1998; Yang and Zhou, 2001; Qiu et al., 2002).

The studied area is located in Jiaodong Peninsula, south to Wulian–Qingdao–Yantai fault (Fig. 1). Lamprophyres are widely distributed in the region as sills, dykes and plug intrusions (e.g., BGMRS, 1991; Cheng et al., 1998; Yang and Zhou, 2001). The lamprophyre samples were mainly collected from Sanjia lode-gold deposit of Rushan County, Yazi and Wanggezhuang villages of Muping County. At the Sanjia gold mine, the lamprophyres occur as dykes in NE to ENE directions, intruding into the country rocks of the gold ore body. Single dykes span a range
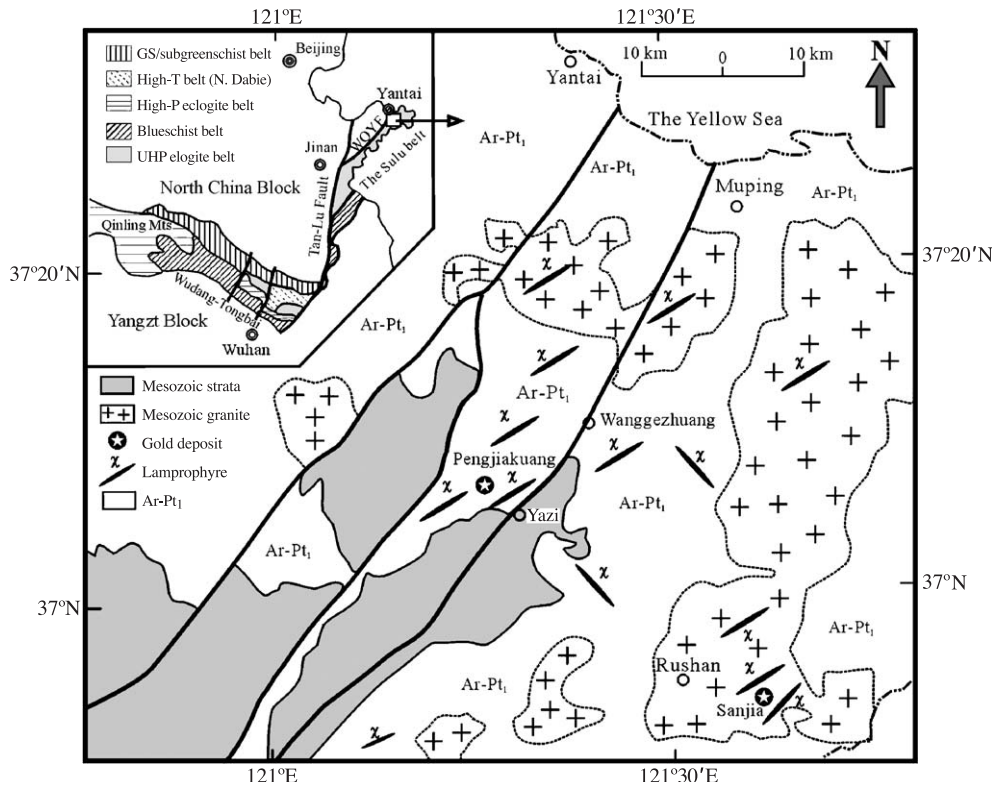
Fig. 1. Geologic map of the Sulu orogen, showing the distribution of early Cretaceous lamprophyres (modified after BGMRS, 1991). Note: lamprophyres from Pengjiakuang lode-gold deposit refer to Cheng et al. (1998); WQYF = Wulian–Qingdao–Yantai fault. Legend as shown in the figure.

of 0.5–15 m in width and 20–150 m in length (Sample 97-3 to 24). Some dykes (Sample 97RS-26, 27) at the locality are intruded into the granitoid plutons at the surface with similar occurrence to those associated with the gold ore bodies. At Yazi and Wanggezhuang (97RY-2 to 25), the lamprophyres occur as dykes, sills and plugs. Both NE- and NW-trending dykes are observed. Single dykes span a width range of 0.3–25 m and 5–200 m in length.

All of the lamprophyre samples are porphyritic with predominant phenocrysts of K-feldspar (0.8–2 mm), plagioclase (1–3 mm), biotite (0.5–3 mm), clinopyroxene (0.5–2 mm), sometimes minor olivine (0.5–1.5 mm) especially in high-MgO samples like 97RS-27 and 97RY-25. The ground mass consists of fine-grained (<0.4 mm grain size) plagioclase, alkali feldspar, biotite, clinopyroxene and minor autogenetic carbonates with accessories like apatite and opaque oxides.

3. Analytical techniques

All samples were crushed to millimeter-scale grain size after removal of weathered rims and handpicked under a magnifier. Only fresh and xen-ocryst- and amygdaloid-free rock chips were selected. These chips were washed in purified water in an ultrasonic bath and crushed in a WC jaw crusher. A split was ground to <160 mesh grain size in an agate ring mill, and this material was used for major- and trace-element analysis. Major-element analysis was carried out by a wet chemical method at Changsha Institute of Geotectonics, Chinese Academy of Sciences (CAS). The analytical errors for major oxides are less than 2%. Trace-element compositions were determined by solution ICP-MS analysis, which were performed using a Perkin-Elmer ELAN 5100 instrument at Macquarie University, Australia. Sample preparations, instrument op-

erating conditions and calibration procedures of the analyses were described by Norman et al. (1998). Conservative estimation of the detection limits is much less than 50 ppb for all elements except for the transition metals and Zr (<100 ppb). The in-house standard Kilauea 93-1489 was analyzed as an unknown to monitor drift and data quality during the period of the analyses. Precision [determined by repeated analysis of Kilauea 93-1489 and presented as relative standard deviation (% RSD) for the period of analysis] is better than 4% for all of the listed elements. Analytical accuracy (presented as average measured value/recommended value) is better than 5%. The total analytical blank is <10 ppb for most elements except for Cr, Ni, Sr and Ba, making blank corrections mostly $<0.1\%$ for the lamprophyre samples.

Sr and Nd isotopic ratios were measured by mass spectrometer VG354 at the Institute of Geology and Geophysics, CAS. Rock chips <20 mesh are used for Sr and Nd isotope analysis. Before being ground to <160 mesh in an agate rill mill and dissolved, these chips were leached in purified 6N HCl for 24 h at room temperature to remove the effect of surface alteration or weathering on Sr isotopic ratios. The Sr and Nd isotope ratios were respectively normalized to $^{86}Sr/^{88}Sr = 0.1194$ and $^{146}Nd/^{144}Nd = 0.7219$. The La Jolla standard yielded $^{143}Nd/^{144}Nd = 0.511862 \pm 10$ ($n = 13$), and NBS987 gave $^{87}Sr/^{86}Sr = 0.710240 \pm 11$ ($n = 6$). The whole procedure blank is less than $2-5 \times 10^{-10}$ g for Sr and 5×10^{-11} g for Nd. Analytical errors for Sr and Nd isotopic ratios were given as 2σ. The $^{87}Rb/^{86}Sr$ and $^{147}Sm/^{144}Nd$ ratios were calculated using the Rb, Sr, Sm and Nd abundance obtained by ICP-MS. The initial $^{87}Sr/^{86}Sr$ and $^{143}Nd/^{144}Nd$ ratios were corrected using a mean K–Ar age of 125 Ma.

K–Ar dating was performed at Guangzhou Institute of Geochemistry, CAS. Whole-rock samples were used after removal of xenocrysts, and biotite separates were handpicked under a binocular with purity >98%. Detailed description of sample preparation and analytical procedure is reported by Fan et al. (2003). The age calculation parameters used are $K^{40} = 0.1167\%$, $K_e = 5.811 \times 10^{-11}$/year and $K_b = 4.962 \times 10^{-10}$/year. The analytical result for Chinese standard ZBH-2506 is 132.3 ± 2.1 Ma (recommended age 132 Ma). K–Ar dating results, major- and trace-element compositions, and Sr and Nd isotope data of early Cretaceous lamprophyres from the Sulu orogen are listed in Tables 1–3, respectively.

4. Results

4.1. Emplacement ages of lamprophyres

Four samples respectively intruded into the country rocks of Sanjia lode-gold deposit (97RS-9 and 97RS-16), Mesozoic granitoid pluton (97RY-2) and late Archean metamorphic basement (97RY-13, biotite concentration) yield K–Ar apparent ages of 126.7 ± 2.0, 122.2 ± 1.8, 126.0 ± 2.0 and 123.5 ± 2.3 Ma, consistent with previous K–Ar dating results of 122–124 Ma (e.g., Yang and Zhou, 2001). These ages are identical to the major gold mineralization and emplacement ages of voluminous granitic magmas (120–130 Ma) in Jiaodong Peninsula (e.g., Qiu et al., 2002; Yang and Zhou, 2001; Wang et al., 1998). Therefore, the widespread emplacement of lamprophyres occurred within the early Cretaceous and was contemporaneous to the regional granitic magmatism and large-scale gold mineralization episodes.

Table 1
K–Ar dating results of lamprophyres in the Sulu orogen, eastern China

Sample	Locality	Wall rock types	Weight (g)	K contents (wt.%)	Radiogenic ^{40}Ar (%)	Radiogenic ^{40}Ar ($\times 10^{-11}$mol)	K–Ar apparent age (Ma)
97RS-9	Sanjia gold deposit	mineralized wall rocks	0.0767 (wr)	3.69 ± 0.06	96.26	6.444	126.7 ± 2.0
97RS-16	Sanjia gold deposit	mineralized wall rocks	0.0571 (wr)	2.63 ± 0.04	84.56	3.292	122.2 ± 1.8
97RY-2	Yazi	Mesozoic granite	0.0705 (wr)	1.75 ± 0.03	77.53	2.793	126.0 ± 2.0
97RY-13	Wanggezhuang	$Ar-Pt_1$ basement rocks	0.0693 (Bi)	4.62 ± 0.07	76.24	3.076	123.5 ± 2.3

wr = whole rock; Bi = biotite separates.

Table 2
Major oxide (wt.%), trace element (ppm) compositions of early Cretaceous lamprophyres in the Sulu orogen, eastern China

Sample	97RS-3	97RS-7	97RS-9	97RS-16	97RS-19	97RS-21	97RS-24	97RS-26	97RS-27	97RY-2	97RY-4	97RY-6	97RY-13	97RY-24	97RY-25
Age (Ma)			127	122						126			127		
SiO_2	55.40	47.94	53.78	50.36	46.80	50.76	55.00	48.64	44.66	53.00	50.28	53.42	52.94	51.36	49.94
Al_2O_3	17.33	15.83	18.62	16.41	15.13	17.84	17.55	16.41	13.41	16.55	14.84	15.13	15.27	14.98	13.98
Fe_2O_3	2.06	1.42	2.48	0.96	3.25	2.77	0.90	1.46	2.05	2.03	2.37	0.91	1.07	2.29	2.33
FeO	3.78	5.89	3.64	5.46	5.52	4.60	4.58	5.86	6.38	4.77	4.96	5.46	5.08	5.05	5.15
CaO	4.98	8.05	7.01	6.62	10.64	6.75	6.49	9.47	11.89	8.44	8.05	7.01	6.62	7.79	8.44
MgO	3.72	8.92	3.11	5.85	8.48	3.77	3.49	7.16	10.51	5.89	7.02	7.68	7.73	7.40	9.14
K_2O	4.02	2.11	3.95	2.89	2.57	4.60	3.48	1.95	2.17	2.27	2.57	2.58	2.72	2.39	2.07
Na_2O	4.20	3.09	4.16	3.55	2.93	4.03	4.34	3.23	2.16	3.40	2.63	2.87	3.25	2.31	2.13
P_2O_5	0.83	0.52	0.60	0.49	0.62	1.16	0.59	0.54	0.90	0.40	0.47	0.38	0.45	0.32	0.29
MnO	0.12	0.13	0.14	0.14	0.15	0.14	0.10	0.13	0.18	0.12	0.14	0.16	0.14	0.12	0.13
TiO_2	1.05	1.05	1.08	0.92	1.28	1.19	0.98	1.16	1.28	0.89	0.97	0.85	0.99	0.88	0.99
LOI	2.58	3.90	1.40	6.27	2.90	2.72	2.76	4.10	4.62	2.61	4.18	3.11	3.88	5.03	5.47
Total	100.07	98.85	99.97	99.92	100.27	100.33	100.26	100.11	100.21	100.37	98.48	99.56	100.14	99.92	100.06
Mg number	54	69	49	62	64	49	54	64	70	62	64	69	70	65	69
Sc	10	24	12	14	32	15	12	21	25	22	23	22	19	22	25
V	95	161	140	137	228	137	103	170	190	149	158	140	137	157	167
Cr	79	473	10	140	277	62	48	295	631	390	411	515	487	410	546
Co	16	37	17	24	34	21	17	32	41	23	32	29	30	35	41
Ni	26	215	11	116	49	28	37	130	190	89	155	157	169	160	216
Rb	104	39.5	84.4	62.9	47.9	87.3	66.8	35.5	65.7	48.4	70.1	54.5	65.8	61.8	69.7
Sr	1162	902	1043	759	1310	1686	980	912	1101	1038	925	1042	847	792	706
Y	17.0	20.9	21.5	16.1	23.8	20.2	17.0	20.6	22.9	18.9	21.5	17.9	19.8	16.2	18.1
Zr	217	180	158	144	130	208	180	137	161	164	170	147	166	99.8	117
Hf	4.86	3.86	3.10	3.04	3.08	4.34	4.28	3.08	3.58	3.93	3.45	3.19	3.63	2.44	2.58
Nb	16.6	12.4	12.7	8.92	6.89	17.3	13.2	11.6	11.6	8.03	9.36	7.53	9.65	6.23	4.56
Ta	0.72	0.62	0.64	0.40	0.31	0.83	0.74	0.58	0.56	0.44	0.43	0.37	0.50	0.31	0.22
U	1.84	0.85	1.17	1.16	1.28	2.18	1.78	0.86	0.95	1.32	1.46	1.13	1.71	0.81	0.90
Th	9.83	4.25	6.18	6.00	6.74	9.89	8.49	4.22	4.64	7.20	8.23	6.73	9.76	4.25	5.81
Ba	2580	1386	3122	1896	2510	3091	2001	1307	3261	1962	1691	2638	2002	1454	1452
La	75.80	44.43	73.73	54.05	69.97	78.11	60.53	44.5	55.38	55.77	64.36	51.72	62.13	38.22	39.18
Ce	142.1	85.47	139.3	100.4	136.4	156.4	112.0	85.90	108.2	103.0	116.8	95.16	113.2	71.5	73.66
Pr	17.00	10.38	16.44	11.92	17.11	19.33	13.1	10.19	14.17	12.22	13.31	10.97	13.73	8.09	8.71
Nd	59.62	37.93	59.62	42.73	66.74	70.86	46.62	38.74	53.35	43.32	46.64	39.01	48.39	29.46	32.4
Sm	9.07	6.31	9.18	6.36	10.77	10.45	7.69	6.93	8.73	7.04	7.32	6.34	7.87	5.28	5.47
Eu	2.93	2.16	3.33	2.21	3.38	3.58	2.46	2.24	3.01	2.28	2.34	2.3	2.45	1.94	1.86
Gd	6.84	5.72	7.38	5.29	8.09	8.62	5.72	6.16	6.73	5.41	6.14	5.09	6.37	4.53	4.77
Tb	0.85	0.78	1.01	0.71	1.05	1.07	0.77	0.82	0.93	0.76	0.80	0.68	0.82	0.63	0.64
Dy	3.40	3.76	4.10	3.00	4.57	4.05	3.43	3.89	4.06	3.51	3.68	3.12	3.67	2.92	3.00
Ho	0.62	0.72	0.73	0.54	0.86	0.69	0.66	0.72	0.77	0.72	0.71	0.61	0.67	0.57	0.61
Er	1.48	1.90	1.82	1.47	2.20	1.74	1.74	1.93	2.04	1.96	1.88	1.64	1.81	1.58	1.68
Yb	1.21	1.66	1.40	1.28	1.76	1.35	1.55	1.59	1.73	1.85	1.67	1.47	1.56	1.22	1.37
Lu	0.15	0.23	0.2	0.18	0.26	0.18	0.23	0.20	0.24	0.28	0.25	0.20	0.21	0.19	0.21
Zr/Hf	44.7	46.6	50.8	47.4	42.2	48.0	42.2	44.3	44.9	41.7	49.3	46.2	45.8	40.9	45.5
Nb/Ta	23.0	20.1	19.8	22.3	22.2	20.9	17.8	20.0	20.7	18.3	21.8	20.4	19.3	20.1	20.7

Mg number = 100 × Mg/[Mg + ΣFe] in atomic ratio; LOI = loss of ignition.

Table 3
Sr and Nd isotope data of the early Cretaceous lamprophyres in the Sulu orogen, eastern China

Sample	Rb (ppm)	Sr (ppm)	$^{87}Rb/^{86}Sr$	$^{87}Sr/^{86}Sr \pm 2\sigma$	$^{87}Sr/^{86}Sr(i)$	Sm (ppm)	Nd (ppm)	$^{147}Sm/^{144}Nd$	$^{143}Nd/^{144}Nd \pm 2\sigma$	$\varepsilon_{Nd}(t)$
97RS-3	104	1162	0.2584	0.709119 ± 20	0.70868	9.07	59.62	0.0920	0.511802 ± 11	− 14.7
97RS-7	39.5	902	0.1268	0.708489 ± 16	0.70827	6.31	37.93	0.1006	0.511871 ± 9	− 13.5
97RS-9	84.4	1043	0.2341	0.708274 ± 18	0.70788	9.18	59.62	0.0931	0.511878 ± 9	− 13.2
97RS-19	47.9	1310	0.1059	0.708694 ± 17	0.70851	10.77	66.74	0.0976	0.511753 ± 9	− 15.7
97RS-21	87.3	1686	0.1498	0.708447 ± 15	0.70819	10.45	70.86	0.0891	0.511894 ± 12	− 12.9
97RS-26	35.5	912	0.1127	0.708135 ± 15	0.70794	6.93	38.74	0.1081	0.511973 ± 15	− 11.6
97RS-26 (dup)				0.708088 ± 15	0.70790				0.511939 ± 10	− 12.3
97RS-27	65.7	1101	0.1726	0.708586 ± 19	0.70837	8.73	53.35	0.0989	0.511738 ± 12	− 16.1
97RS-27 (dup)				0.708586 ± 18	0.70829				0.511760 ± 15	− 15.6
97RY-2	48.4	1038	0.1348	0.709126 ± 15	0.70889	7.04	43.32	0.0982	0.511681 ± 13	− 17.2
97RY-2 (dup)				0.709102 ± 18	0.70887				0.511678 ± 11	− 17.2
97RY-4	70.1	923	0.2193	0.70925 ± 20	0.70888	7.32	46.64	0.0949	0.511794 ± 13	− 14.9
97RY-6	54.5	1042	0.1513	0.709600 ± 20	0.70934	6.34	39.01	0.0982	0.511703 ± 13	− 16.7
97RY-13	65.8	847	0.2249	0.709479 ± 18	0.70910	7.87	48.39	0.0983	0.511768 ± 9	− 15.5
97RY-24	61.8	792	0.2258	0.709022 ± 25	0.70864	5.28	29.46	0.1083	0.511713 ± 13	− 16.7
97RY-24 (dup)				0.709072 ± 18	0.70869				0.511698 ± 9	− 17.0

The Rb, Sr, Sm and Nd abundances are measured by ICP-MS, and initial $^{87}Sr/^{86}Sr(i)$ and $\varepsilon_{Nd}(t)$ are calculated using a mean K–Ar age of 125 Ma. dup: duplicate analysis.

4.2. Major and trace elements

The early Cretaceous Sulu orogen lamprophyres span wide range of SiO_2 (46.72–56.83%) and MgO (3.16–10.99%) with Mg numbers of 49–70, similar to potassium-rich lamprophyres reported by Cheng et
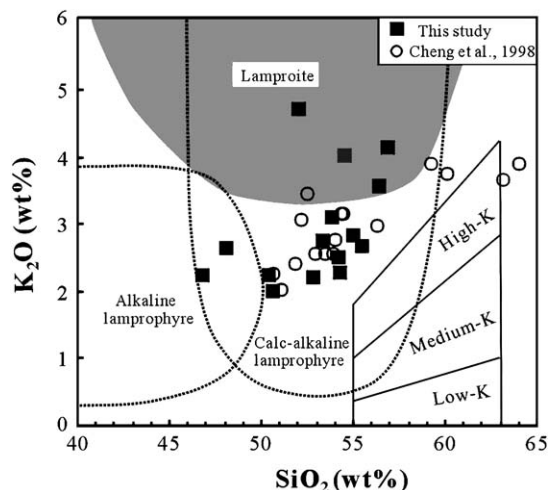

Fig. 2. SiO_2 vs. K_2O plots for rock classification. The lamprophyre classification scheme refers to Rock (1987). Filled square: this study; open circle: Cheng et al. (1998).

al. (1998). They are calc-alkaline lamprophyres according to Rock's (1987) classification scheme in a K_2O vs. SiO_2 diagram (Fig. 2).

Systematic correlations between MgO and major oxides and trace elements suggest an important role of fractional crystallization en route to the surface (Fig. 3). Positive correlations between MgO and FeO_t and other compatible elements like Cr, Ni and negative correlations of MgO vs. Al_2O_3, CaO and SiO_2 are observed (Fig. 3). The abundances of large ion lithophile elements (LILEs) like Rb, Ba, Sr, Th and high-field-strength elements (HFSEs) such as Nb, Zr and Ti and P increase moderately as MgO decreases.

All of the Sulu orogen lamprophyres exhibit sub-parallel chondrite-normalized REE patterns with LREE abundances >100 times and HREE <10 times as chondrite (Fig. 4a), presumably indicating the presence of residual garnet in the melting source (e.g., McKenzie and O'Nions, 1991). These rocks also show slightly positive Eu anomalies (Eu/Eu* = 1.0–1.2). In the primitive mantle-normalized spidergrams, these rocks show significant enrichment in LILE, REE relative to HFSE (Fig. 4b), such as high Ba/Nb, La/Nb, Sm/Zr and Eu/Ti values. Radioactive elements like U and Th show moderate depletion with
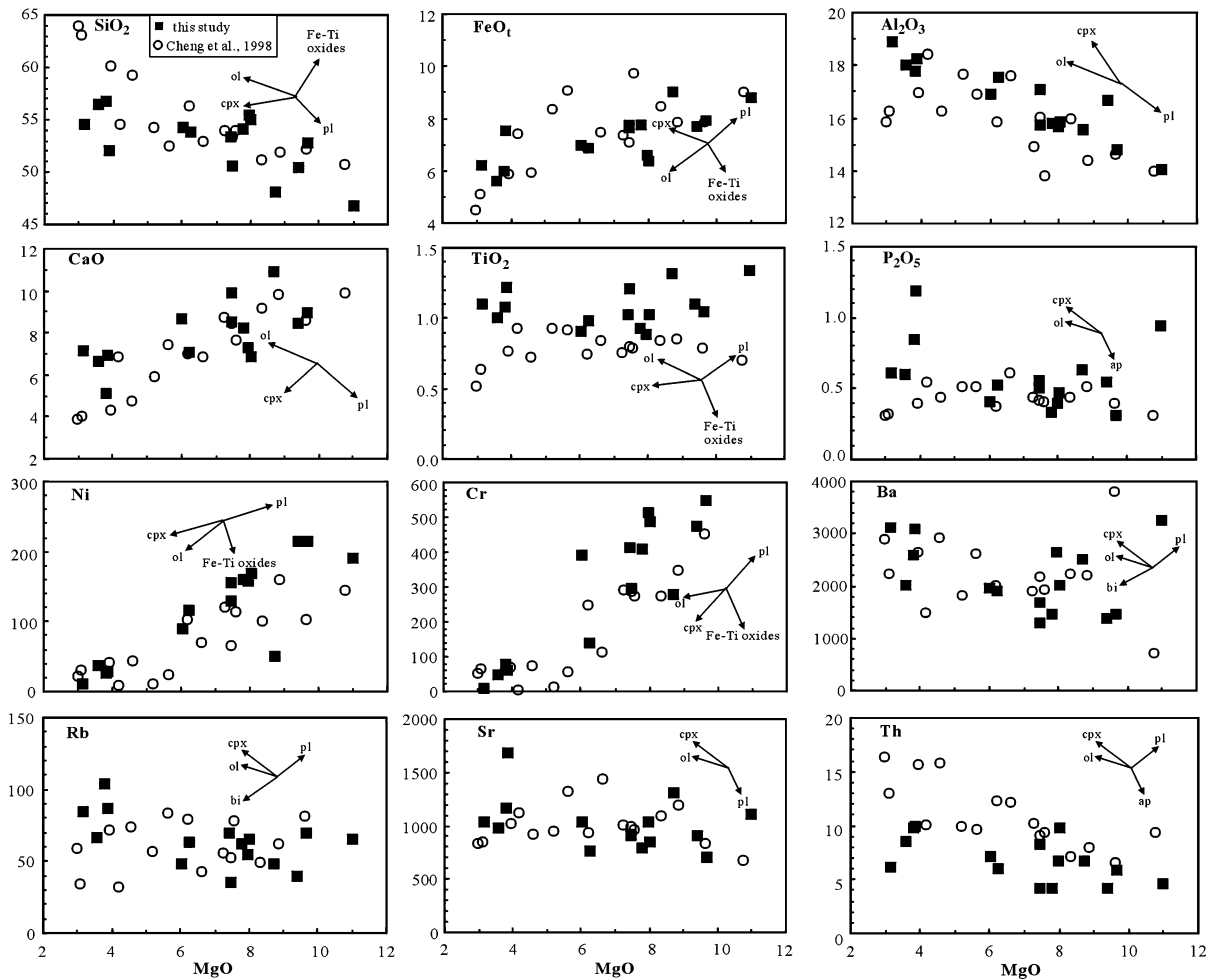
Fig. 3. MgO vs. major- and trace-element diagrams of the Sulu orogen lamprophyres, showing the possible fractional phases during magma evolution. Legends are the same as in Fig. 2.

regard to Ba and La. All studied samples show moderate Nb/Ta and Zr/Hf fractionations and have superchondritic Zr/Hf (39.8–39.8–50.8 with regard to 36 for PM) and Nb/Ta (17.8–23.0, compared with 17.5 for PM) ratios (Sun and McDonough, 1989).

4.3. Sr–Nd isotopes

Sr–Nd isotope data for 12 lamprophyre samples are listed in Table 3. These rocks span an $^{87}Sr/^{86}Sr$ range of 0.70814–0.70960 and $^{143}Nd/^{144}Nd$ range of 0.511681–0.511973. Age-corrected initial $^{87}Sr/^{86}Sr$ ratios are 0.70787–0.70934 and $\varepsilon_{Nd}(t)$ of − 17.2 to − 11.6. As shown in Fig. 5, such isotopic signatures are

similar to lamprophyres at Linglong Gold deposit (Yang and Zhou, 2001), early Cretaceous basaltic lavas in the Sulu orogen (Fan et al., 2001; our unpublished data), but completely different from the Neogene mantle xenolith-bearing basalts (Zhi et al., 1994). The highly enriched Sr and Nd isotope data on these rocks suggest LILE- and LREE-enriched mantle sources in their origin.

5. Discussion

Partial melting of mantle material previously enriched in incompatible elements is considered as
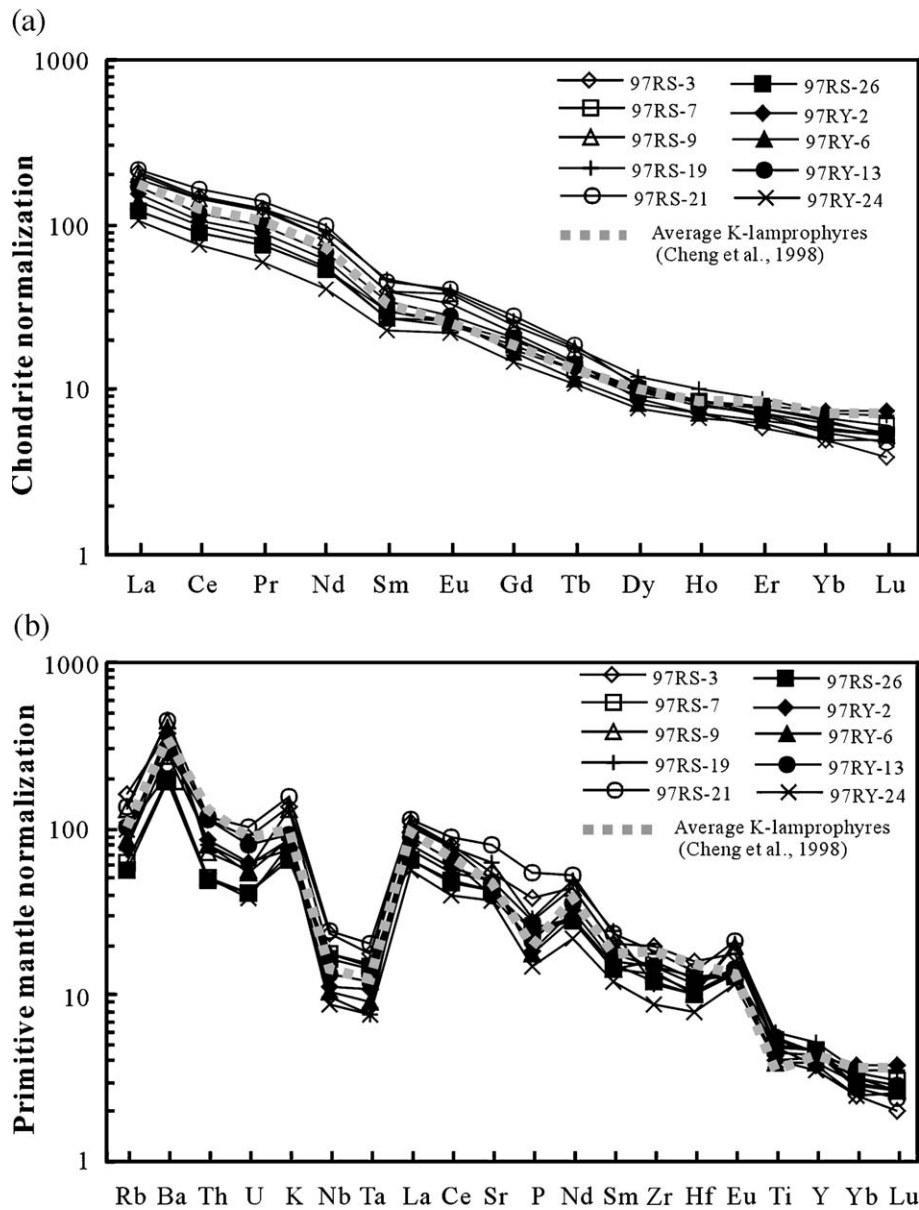
Fig. 4. Chondrite-normalized REE patterns (a) and primitive mantle-normalized spidergrams (b) of the lamprophyres in the Sulu orogen. Data sources: chondrite (Taylor and McLennan, 1985), primitive mantle (Sun and McDonough, 1989), the average trace-element abundances of lamprophyres from Pengjiakuang gold deposit (Cheng et al., 1998).

the most likely explanation for the origin of primary magmas for lamprophyres (e.g., Rock, 1987; Müller and Groves, 1995). The systematic geochemical variations of the Sulu orogen lamprophyres suggest an important role of magma differentiation, whereas the

highly enriched Sr–Nd isotopic signatures and moderate Zr/Hf and Nb/Ta fractionations call for unusual enrichment processes in the source prior to magma generation. In the following text, we will focus on the role of magmatic processes like fractional crystalliza-
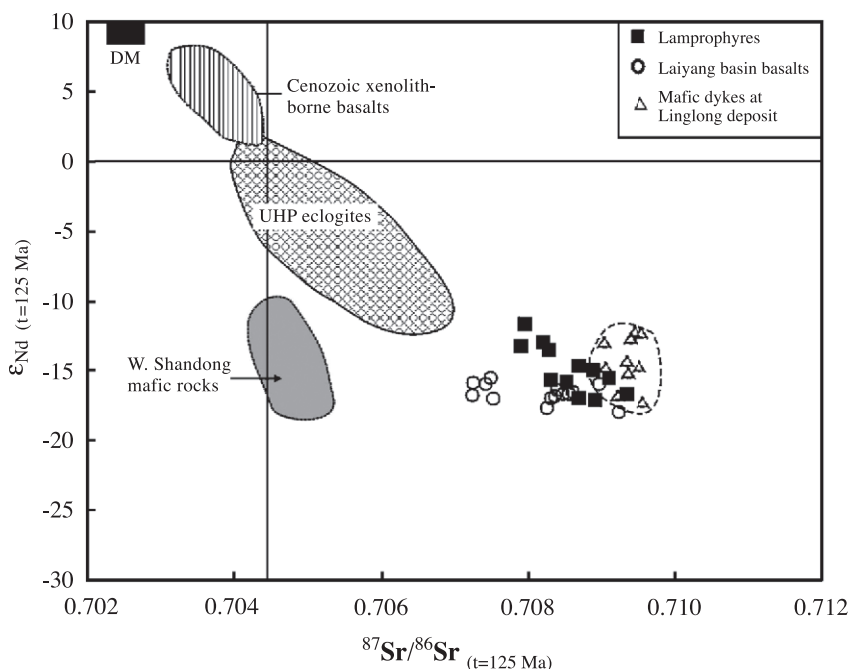
Fig. 5. Sr vs. Nd isotope variation diagram of early Cretaceous Sulu orogen lamprophyres. Data source: UHP eclogites (Jahn et al., 1999, and references therein), W. Shandong mafic rocks (Guo et al., 2001, 2003), Laiyang basin basalts (Fan et al., 2001; our unpublished data), N-Q basalts (Zhi et al., 1994), mafic dykes from Linglong gold deposit (Yang and Zhou, 2001). Legends as shown in the figure.

tion (FC) and crustal contamination, source mineralogy for the lamprophyres and mantle enrichment processes beneath the Sulu orogen.

5.1. Magmatic differentiation

The systematic variation trends between MgO and major and trace elements and the subparallel REE patterns indicate an important role of FC during magma evolution. Olivine is a major fractional phase to account for the rapid decrease in Ni and FeO_t and increase in SiO_2 (Fig. 3). As can be seen in Fig. 3, clinopyroxene fractionation is also important to account for the positive correlations of CaO and Cr vs. MgO, whereas plagioclase differentiation is insignificant according to the negative correlations between MgO and Al_2O_3 and Sr. Crystal fractionation of accessory minerals such as apatite and Fe–Ti oxides are insignificant because of the less variable P_2O_5 and TiO_2 contents. As a whole, a fractional mineral assemblage of ol + cpx ± pl can roughly explain the chemical variation trends in the calc-alkaline lamprophyres in the Sulu orogen.

Crustal contamination might cause significant depletion in Nb–Ta and highly enriched Sr–Nd isotopic signatures in basaltic rocks. The depletion in Th and U relative to La in the primitive mantle-normalized spidergrams rule out the possibility of significant upper–middle crustal contamination (Taylor and McLennan, 1985). Thus, if crustal contamination had occurred, the likely candidate might had been lower crust that developed time-integrated radiogenic Sr–Nd isotopic compositions. In this case, addition of lower crust rocks with relatively lower Sr abundance (e.g., 350 ppm, Rudnick and Fountain, 1995) would cause a Sr decrease in the melts, in contrast with the magma differentiation trend (Fig. 3), in which Sr increases moderately following MgO decrease. On the other hand, the random variations of $^{87}Sr/^{86}Sr(i)$ and $\varepsilon_{Nd}(t)$ vs. MgO tend to suggest source heterogeneity instead of significant contamination by crustal rocks (Fig. 6). In summary, the effect of crustal contamination on magma evolution of the lamprophyres may be limited and their geochemical and isotopic signatures were mainly inherited from LILE- and LREE-enriched but heterogeneous mantle sources.
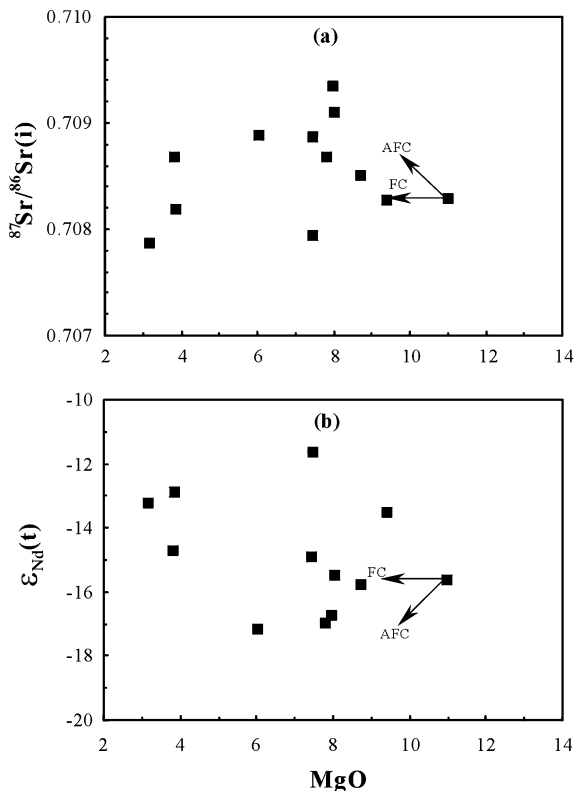
Fig. 6. MgO vs. $^{87}Sr/^{86}Sr(i)$ and $\varepsilon_{Nd}(t)$ diagrams of early Cretaceous Sulu orogen lamprophyres. Note that the random variations in Sr and Nd isotope data following MgO decrease indicate insignificant crustal contamination during magma evolution. FC = fractional crystallization; AFC = assimilation and fractional crystallization.

5.2. Source mineralogy

The high MgO (e.g., 97RS-27, MgO = 11%) and compatible element contents like Cr (631 ppm) and Ni (190 ppm) in some lamprophyre samples can roughly represent primary mantle-derived melts, which makes it possible to characterize the source mineralogy. A signature of residual garnet at the time of melting is evident from the low HREE concentrations (< 10 times as chondrite) and very high LREE abundances (>100 times as chondrite) (McKenzie and O'Nions, 1991; Polat et al., 1997; Furman and Graham, 1999).

As mentioned above, the significant LILE and LREE enrichment and HFSE depletion in the PM-normalized spidergrams (Fig. 4b) and highly enriched

Sr–Nd isotopic signatures (Table 3) in the rocks call for a LILE- and LREE-enriched mantle source in their origin, where volatile-bearing mineral assemblage such as phlogopite and amphibole is responsible for radiogenic Sr evolution (Fig. 7). It has been suggested that phlogophite and amphibole are the major repositories for LILE in lithospheric mantle (e.g., Foley et al., 1996; Ionov et al., 1997; Grégoire et al., 2000a). With regard to amphibole, phlogopite has much higher partition coefficients for Rb, Ba but lower for Sr than amphibole; thus, the high Rb/Sr and low Ba/Rb ratios as well as negative correlation between the two pairs of elemental ratios in these rocks indicate a predominance of phlogopite rather than amphibole in the melting source (Fig. 7). Probably, the mantle source for early Cretaceous Sulu orogen lamprophyres was mainly composed of phlogopite garnet peridotites.

5.3. Mantle enrichment processes beneath the Sulu orogen

The high concentrations of incompatible elements and high $^{87}Sr/^{86}Sr$ but low $^{143}Nd/^{144}Nd$ ratios in the Sulu orogen lamprophyres call for a LILE and LREE enrichment process before or during magma generation. Two kinds of metasomatism might be responsible for such geochemical and isotopic signatures: (1) a recent subduction-related metasomatic event by fluid/melt derived from an ancient continental crust that developed extremely enriched Sr–Nd isotopic signatures (e.g., Jahn et al., 1999; Fan et al., 2001); and (2) an old metasomatic event by LILE and LREE-enriched melt/fluid that usually happens in subcratonic lithospheric mantle (e.g., Menzies et al., 1987), where asthenosphere-derived small fractional melts interacted with wall peridotites to form metasomatized rocks, such as that documented by early Cretaceous mafic magmatism within the North China Block (Guo et al., 2001, 2003).

The characteristic moderate Zr/Hf and Nb/Ta fractionations (Table 2) in early Cretaceous calc-alkaline lamprophyres cannot be simply explained by analytical errors, but probably imply an unusual metasomatic assemblage during the formation of the mantle source. Both Nb and Ta show similar geochemical behaviors due to their nearly identical ionic radii and charge (Jochum et al., 1986, 1989), so Nb/Ta value is hardly affected by magmatic processes

such as fractional crystallization and partial melting unless a significant volume of rutile and/or low-Mg-number amphibole is involved in the mantle source (e.g., Ionov et al., 1997; Foley et al., 2000, 2002; Tiepolo et al., 2001). Partition coefficients for rutile/melt from both experimental and natural systems suggest that rutile is a potential phase to fractionate Nb from Ta and produce superchondritic Nb/Ta value in the melt (Foley et al., 2000, 2002). Hence, melt coexistent with residual rutile at the time of melting will have superchondritic rather than sub-chondritic Nb/Ta value. However, if rutile is a metasomatic mineral extracted from the metamorphic rocks such as the UHP rocks, then the resulting metasomatized mantle source will have superchon-dritic Nb/Ta value. Mass consideration indicates that if only 0.1% rutile is added into the mantle, Nb/Ta ratio in the metasomatized source would be increased by about 40–60%. On the other hand, amphibole of low Mg number (e.g., titanian pargasite and kaersu-tite) is another phase to fractionate Nb from Ta (Tiepolo et al., 2001; Foley et al., 2002; Grégoire et al., 2000a,b). Generally, amphibole in mantle peridotites generally shows high Mg number (>70) and melting of amphibole-bearing peridotites could not successfully produce melts with low Nb/Ta ratios

(e.g., Foley et al., 2002). In addition, the low Ba/Rb and high Rb/Sr ratios (Fig. 7) also preclude a significant volume of amphibole in the melting source. We thus attribute the superchondrititc Nb/Ta ratios in the Sulu orogen lamprophyres to a rutile-rich metasomatism, during which rutile had been extracted from the UHP rocks and led to high Nb/Ta value in the source of the lamprophyres.

Similarly, because of very similar geochemical behavior between Zr and Hf (Jochum et al., 1986, 1989), Zr/Hf ratio remains constant during petroge-netic processes except for fluid metasomatism (e.g., Dupuy et al., 1992; Rudnick et al., 1993). The super-chondritic Zr/Hf ratios in these lamprophyres suggest a metasomatized mantle origin. It is generally supposed that the elevated Zr/Hf value is closely associated with an enrichment process by small-volume carbonate-rich metasomatic melts/fluids (e.g., Rudnick et al., 1993; Dupuy et al., 1992; Furman and Graham, 1999). These rocks also show significant enrichment in REE relative to HFSE (e.g., Eu/Ti; Fig. 4b). All of these signatures are characteristics of carbonatite metasomatism (Dupuy et al., 1992; Rudnick et al., 1993) and suggest that the source region for these lamprophyres had been infiltrated by carbonate-rich magmas (Furman and Graham, 1999). Therefore, the observed Zr/Hf and
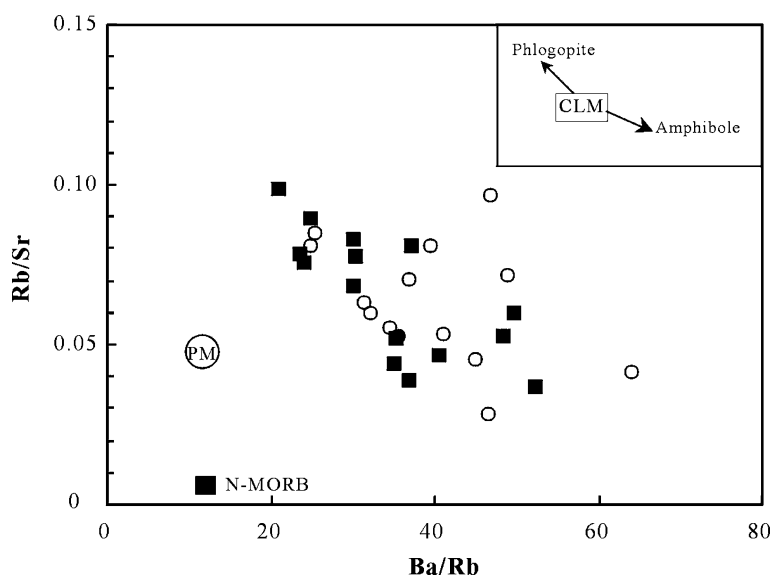

Fig. 7. Rb/Sr vs. Ba/Rb diagram of early Cretaceous lamprophyres in the Sulu orogen, suggesting a predominant volatile-bearing phases of phlogophite rather than amphibole in the source. Legends are the same as in Fig. 2.

Nb/Ta fractionations in these rocks favored a rutile-
and carbonate-rich metasomatic assemblage as that
documented in off-cratonic and oceanic peridotite
xenoliths (e.g., Ionov et al., 1999; Grégoire et al.,
2000b), in good agreement with the presence of
clinopyroxene, rutile and apatite exsolutions in garnet
from the UHP rocks (Ye et al., 2000), which suggested
that rutile and apatite might have been dissolved from
the UHP eclogites and involved in the metasomatic
melts during the subduction and/or exhumation of the
continental slabs.

In the Dabie–Sulu orogenic belt, features such as
moderate Zr/Hf and Nb/Ta fractionations (Fig. 8) and
highly enriched Sr–Nd isotopic signatures are preva-
lent in early Cretaceous mafic volcanic rocks, such as
basaltic trachyandesites from the northern Dabie oro-
gen (Fan et al., 2004), the basaltic lavas in Laiyang
basin (our unpublished data) and along the Sulu
orogen (Fan et al., 2001). Therefore, it appears that
carbonate- and rutile-rich metasomatic assemblage
may be common beneath the Dabie–Sulu continental
collisional belt.

5.4. Conditions for carbonate- and rutile-rich meta-somatism beneath the Sulu orogen

It is generally considered that carbonate-rich melts/
fluids are generated at high pressure by low-degree
melting of mantle sources (e.g., 5–6 GPa; Dalton and
Presnall, 1998; Ryabchikov et al., 1993). Additionally,
amphibole and phlogophite are common volatile meta-
somatic phases in metasomatized mantle (e.g., Ionov et
al., 1997; Grégoire et al., 2000a), so the absence of
amphibole in the melting source possibly reflect that
the early Cretaceous lithosphere in the Sulu orogen
was so thick (e.g., >100 km, Olafsson and Eggler,
1983) that amphibole was still unstable in response to
thermal erosion of the underlying convective mantle.
This suggests that the metasomatic melts were gener-
ated at much greater depths than the stability filed of
amphibole. All these facts suggest that the carbonate-
and rutile-rich metasomatic event occurred under high
pressures, consistent with the deep continental sub-
duction documented by the UHP rocks (e.g., Cong,
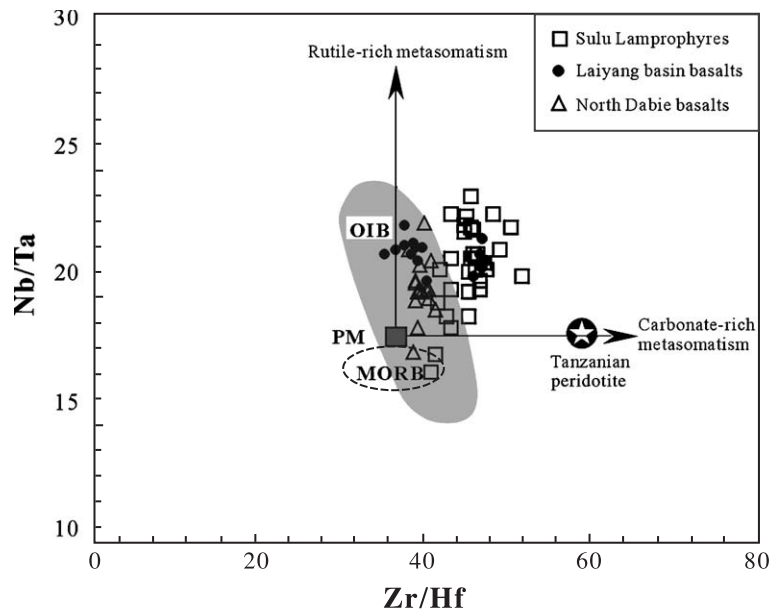1996; Ye et al., 2000; Jahn et al., 1996). The remaining

Fig. 8. Zr/Hf vs. Nb/Ta plots of early Cretaceous lamprophyres in the Sulu orogen and contemporaneous basaltic rocks from the Dabie–Sulu belt, showing possible enrichment processes in the source. Data source: mean Tanzanian peridotites (Rudnick et al., 1993); range of MORB (Sun and McDonough, 1989); range of OIB (Foley et al., 2002; Rudnick et al., 2000), Laiyang basin basalts (our unpublished data) and the north Dabie basalts (Fan et al., 2004). The hypothetical Zr/Hf ratio for eclogites and MORB and Nb/Ta ratios for Tanzanian peridotites are chondritic. The moderate Zr/Hf and Nb/Ta fractionations indicate a metasomatism by carbonate- and rutile-rich assemblage before magma generation. Legends as shown in the figure.

question is what kinds of possible mechanisms are possible for the enrichment processes beneath the Sulu orogen.

One possible mechanism for the metasomatic event may be similar to that occurring in the case of subduction of oceanic slabs, where fluid/melt metasomatism is commonly ascribed to dehydration or melting of the subducted slabs. However, evidence from C and O stable isotope geochemistry of the HP-UHP rocks in the Dabie–Sulu belt suggests that dehydration and/or melting was insignificant during the subduction of the Yangtze lithosphere and formation of the HP-UHP rocks (Zheng et al., 2003, and references therein). In this respect, the carbonate- and rutile-rich melt metasomatism beneath the Sulu orogen was unlikely to have been simultaneous to continental subduction. Alternatively, seismic investigations on the Dabie–Sulu belt and U–Pb dating results of collision-related K-rich complex from the Sulu orogen suggested that slab breakoff occurred after the Triassic collision (Xu et al., 1999; Chen et al., 2003), which could be a likely mechanism for the metasomatic event. Following slab breakoff, asthenospheric upwelling and lithospheric extension caused the rapid exhumation of the UHP terranes (e.g., Li et al., 1999) and would provide heat supply to melt the trapped subducted continental crust. These melts then interacted with the wall lock peridotites to form the metasomatized mantle lithosphere beneath the Dabie–Sulu belt.

6. Concluding remarks

Early Cretaceous (122–127 Ma) calc-alkaline lamprophyres from the Sulu orogen in eastern China show significant LILE and LREE enrichment, Nb–Ta depletion and highly enriched Sr–Nd isotopic signatures. The characteristic moderate Zr/Hf and Nb/Ta fractionations favor a metasomatic event by carbonate- and rutile-rich assemblage at high pressures, probably as a result of slab breakoff and the induced low-degree melting of the trapped subducted continental crust, different from that generally occurs in the case of the subduction of oceanic slabs, where metasomatism is commonly ascribed to dehydration and/or melting of the subducted slabs. These rocks were derived from decompression melting of such enriched mantle sources that were mainly composed

of phlogopite garnet peridotites and experienced strong fractional crystallization of olivine + clinopyroxene ±plagioclase en route to the surface. Furthermore, the similar geochemical and isotopic signatures in both the Sulu orogen lamprophyres and the contemporaneous mafic rocks in the Dabie–Sulu HP-UHP terranes suggest predominant enrichment processes by carbonate- and rutile-rich metasomatic assemblage underneath the continental collisional belt.

References

Amelin, Y.V., Neymark, L.A., Ritsk, E.Y., Nemchin, A.A., 1996. Enriched Nd–Sr–Pb isotopic signatures in the Dovyren layered intrusion (eastern Siberia, Russia): evidence for source contamination by ancient upper-crust material. Chem. Geol. 129, 39–69.

Arculus, R.J., 1994. Aspects of magma genesis in arcs. Lithos 33, 189–208.

Bureau of Geology and Mineral Resources of Shandong Province (BGMRS), 1991. Regional Geology of Shandong Province. Geological Publishing house, Beijing (594 pp., in Chinese).

Cao, G., Wang, Z., Zhang, C., 1990. The Jiaonan terrane in Shandong Province and the tectonic significance of Wulian–Rongcheng fault. Shandong Geol. 6, 1–15 (in Chinese).

Chen, J.F., Xie, Z., Li, H.M., Zhang, X.D., Zhou, T.X., Park, Y.S., Ahn, K.S., Chen, D.G., Zhang, X., 2003. U–Pb zircon ages for a collision-related K-rich complex at Shidao in the Sulu ultrahigh pressure terrane. China Geochem. J. 37, 33–46.

Cheng, X., Cheng, J., Wang, J., 1998. Element geochemistry of shoshonitic lamprophyres in the Pengjiakuang gold district, Shandong Province, China. Geochimica 27, 91–100 (in Chinese with English abstract).

Cong, B.L. (Ed.), 1996. Ultrahigh-Pressure Metamorphic Rocks in the Dabie–Sulu Region of China. Science Press. Beijing: China and Kluwer Academic Publishing, Dordrecht, 224 pp.

Dalton, J.A., Presnall, D.C., 1998. The continuum of primary carbonatitic–kimberlitic melt compositions in equilibrium with lherzolite: data from the system $CaO–MgO–Al_2O_3–SiO_2–CO_2$ at 6 GPa. J. Petrol. 39, 1953–1964.

Dupuy, C., Liotard, J.M., Dostal, J., 1992. Zr/Hf fractionation in intraplate basaltic rocks: carbonate metasomatism in the mantle source. Geochim. Cosmochim. Acta 56, 2417–2423.

Fan, W.M., Guo, F., Wang, Y.J., Lin, G., Zhang, M., 2001. Post-orogenic bimodal volcanism along the Sulu orogenic belt in eastern China. Phys. Chem. Earth 27, 733–746.

Fan, W.M., Guo, F., Wang, Y.J., Lin, G., 2003. Late Mesozoic calc-alkaline volcanism of post-orogenic extension in the northern Da Hinggan Mountains, northeastern China. J. Volcanol. Geotherm. Res. 121, 115–135.

Fan, W.M., Guo, F., Wang, Y.J., Zhang, M., 2004. Geochemistry of late Mesozoic volcanism in the northern Huaiyang tectono-magmatic belt, central China: partial melts from a lithospheric mantle with subducted continental crust relicts beneath the Dabie orogen? Chem. Geol., in press.

Foley, S.F., Jackson, S.E., Fryer, J.D., Greenough, G.A.J., 1996. Trace element partition coefficients for clinopyroxene and phlogophite in an alkaline lamprophyre from Newfoundland by LAM-ICP-MS. Geochim. Cosmochim. Acta 60, 629–638.

Foley, S.F., Barth, M.G., Jenner, G.A., 2000. Rutile/melt partition coefficients for trace elements and an assessment of the influence of rutile on the trace element characteristics of subduction zone magmas. Geochim. Cosmochim. Acta 64, 933–938.

Foley, S., Tiepolo, M., Vannucci, R., 2002. Growth of early continental crust controlled by melting of amphibolite in subduction zones. Nature 417, 837–840.

Furman, T., Graham, D., 1999. Erosion of lithospheric mantle beneath the East African Rift system: geochemical evidence from the Kivu volcanic province. Lithos 48, 237–262.

Grégoire, M., Lorand, J.P., O'Reilly, S.Y., Cottin, J.Y., 2000a. Armalcolite-bearing, Ti-rich metasomatic assemblages in harzburgitic xenoliths from the Kerguelen Islands: implications from the oceanic mantle budget of high-filed strength elements. Geochim. Cosmochim. Acta 64, 673–694.

Grégoire, M., Moine, B.N., O'Reilly, S.Y., Cottin, J.Y., Giret, A., 2000b. Trace element residence and partitioning in mantle xenoliths metasomatized by highly alkaline, silicate- and carbonate-rich melts (Kerguelen Islands, Indian Ocean). J. Petrol. 41, 477–509.

Guo, F., Fan, W.M., Wang, Y.J., Lin, G., 2001. Late Mesozoic mafic intrusive complexes in the North China Block: constraints on the nature of subcontinental lithospheric mantle. Phys. Chem. Earth 26, 759–771.

Guo, F., Fan, W.M., Wang, Y.J., Lin, G., 2003. Geochemistry of late Mesozoic mafic magmatism in west Shandong Province, eastern China: characterizing the lost lithospheric mantle beneath the North China Block. Geochem. J. 37, 63–77.

Hunter, A.G., Blake, S., 1995. Petrogenetic evolution of a transitional tholeiitic-calc-alkaline series: Towada volcano, Japan. J. Petrol. 36, 1579–1605.

Ionov, D.A., O'Reilly, S.Y., Griffin, W.L., 1997. Volatile-bearing minerals and lithophile trace elements in the upper mantle. Chem. Geol. 141, 153–184.

Ionov, D.A., Gregoire, M., Prikhod'ko, V.S., 1999. Feldspar–Ti-oxide metasomatism in off-cratonic continental and oceanic upper mantle. Earth Planet. Sci. Lett. 165, 37–44.

Jahn, B.M., Cornichet, J., Cong, B.L., Yui, T.F., 1996. Ultrahigh-ε_{Nd} eclogites from an ultrahigh-pressure metamorphic terrane of China. Chem. Geol. 127, 61–79.

Jahn, B.M., Wu, F.Y., Lo, C.-H., Tsai, C.H., 1999. Crust–mantle interaction induced by deep subduction of the continental crust:: Geochemical and Sr–Nd isotopic evidence from post-collisional mafic–ultramafic intrusions of the northern Dabie complex, central China. Chem. Geol. 157, 119–146.

Jochum, K.P., Seufret, H.M., Spettel, B., Palme, H., 1986. The solar-system abundances of Nb, Ta, and Y, and the relative abundances of refractory lithophile elements in differentiated planetary bodies. Geochim. Cosmochim. Acta 50, 1173–1183.

Jochum, K.P., McDonough, W.F., Palme, H., Spettel, B., 1989. Compositional constraints on the continental lithospheric mantle from trace elements in spinel peridotite xenoliths. Nature 340, 548–550.

Li, S.G., Jagoutz, E., Lo, C.-H., Chen, Y.Z., Li, Q.L., 1999. Sm/Nd, Rb/Sr and $^{40}Ar/^{39}Ar$ isotopic systematics of the ultrahigh-pressure metamorphic rocks in the Dabie–Sulu belt central China: a retrospective view. Int. Geol. Rev. 41, 1114–1124.

McKenzie, D.P., O'Nions, R.K., 1991. Partial melt distributions from rare-earth element concentrations. J. Petrol. 32, 1021–1091.

Menzies, M.A., Rogers, N., Tindle, A., Hawkesworth, C.J., 1987. Metasomatic and enrichment processes in lithospheric peridotites, an effect of asthenosphere–lithosphere interaction. In: Menzies, M.A., Hawkesworth, C.J. (Eds.), Mantle Metasomatism. Academic Press, London, pp. 313–361.

Müller, D., Groves, D.I., 1995. Potassic Igneous Rocks and Associated Gold–Copper Mineralization Springer-Verlag (210 pp.).

Norman, M.D., Griffin, W.L., Pearson, N.J., Garcia, M.O., O'Reilly, S.Y., 1998. Quantitative analysis of trace element abundances in glasses and minerals: a comparison of laser ablation inductively coupled plasma mass spectrometry, solution inductively coupled plasma mass spectrometry, proton microprobe and electron microprobe data. J. Anal. At. Spectrom. 13, 477–482.

Olafsson, M., Eggler, D.H., 1983. Phase relation of amphibole, phlogophite carbonate and phlogophite carbonate peridotite: petrological constraint on the asthenosphere. Earth Planet. Sci. Let. 64, 305–315.

Polat, A., Kerrich, R., Casey, J.F., 1997. Geochemistry of Quaternary basalts erupted along the east Anatolian and Dead Sea fault zones of Southern Turkey: implications for mantle sources. Lithos 40, 55–68.

Qiu, Y.M., Groves, D.I., McNaughton, N.G., Wang, L.G., Zhou, T.H., 2002. Nature, age, and tectonic setting of granitoid-hosted, orogenic gold deposits of the Jiaodong Peninsula, eastern North China Craton, China. Mineral. Deposita 37, 283–305.

Rock, N.M.S., 1987. The nature and origin of lamprophyres: an overview. In: Fitton, J.G., Upton, B.G.J. (Eds.), Alkaline Igne-

ous Rocks. Geol. Soc. Spec. Pub., vol. 30. Blackwell, London, pp. 191–226.

Rudnick, R.L., Fountain, D.M., 1995. Nature and composition of the continental crust: a lower crustal perspective. Rev. Geophys. 33, 267–309.

Rudnick, R.L., McDonough, W.F., Chapell, B.W., 1993. Carbonatite metasomatism in the northern Tanzanian mantle: petrographic and geochemical characteristics. Earth Planet. Sci. Lett. 114, 463–475.

Rudnick, R.L., Barth, M., Horn, I., McDonough, W.F., 2000. Rutile-bearing refractory eclogites: missing link between continent and depleted mantle. Science 287, 278–281.

Ryabchikov, I.D., Brey, G.P., Bulatov, V.K., 1993. Carbonate melts coexisting with mantle peridotites at 50 kb. Petrology 1, 159–163.

Sun, S.S., McDonough, W.F., 1989. Chemical and isotopic systematics of oceanic basalts: implication for mantle composition and processes. In: Saunder, A.D., Norry, M.J. (Eds.), Magmatism in the Ocean Basins. Geol. Soc. Spec. Pub., vol. 42, pp. 313–345.

Taylor, S.R., McLennan, S.M. 1985. The Continental Crust: Its Composition and Evolution. Blackwell, Oxford Press, 312 pp.

Tiepolo, M., Vannucci, R., Oberti, R., Foley, S., Bottazzi, P., Zanetti, A., 2000. Nb and Ta incorporation and fractionation in titanian pargasite and kaersutite: crystal-chemical constraints and implications for natural systems. Earth Planet. Sci. Lett. 176, 185–201.

Tiepolo, M., Bottazzi, P., Foley, S.F., Oberti, R., Zanetti, A., 2001. Fractionation of Nb and Ta from Zr and Hf at mantle depths: the role of titanian–pargasite and kaersutite. J. Petrol. 42, 221–232.

Turner, S., Arnaud, N., Liu, J., Hawkesworth, C.J., Harris, N., Kelley, S., van Calsteren, P., Peng, W., 1996. Post-collision, shoshonitic volcanism on the Tibetan Plateau: implications for convective thinning of the lithosphere and the source of oceanic basalts. J. Petrol. 37, 45–71.

Wang, L.G., Qiu, Y.M., McNaughton, N.G., Groves, D.I., Luo, Z.K., Huang, J.Z., Miao, L.C., Liu, Y.K., 1998. Constraints on crustal evolution and gold metallogeny in the northeastern Jiaodong Peninsula, China, from SHRIMP U–Pb zircon studies of granitoids. Ore Geol. Rev. 13, 275–291.

Xu, S., Okay, A.I., Sengor, A.M.C., Su, W., Liu, Y., Jiang, L., 1992. Diamond from Dabie Shan eclogites and its implication for tectonic setting. Science 256, 80–82.

Xu, P.F., Sun, R.M., Liu, F.T., Wang, Q.C., Cong, B.L., 1999. The subduction and slab breakoff in the Dabie–Sulu belt: evidence from the seismological chromatography. Chin. Sci. Bull. 44, 1658–1661 (in Chinese).

Yang, J.H., Zhou, X.H., 2001. Rb–Sr, Sm–Nd, and Pb isotope systematics of pyrite: implications for the age and genesis of lode gold deposits. Geology 29, 711–714.

Ye, K., Hirajima, T., Ishiwateri, A., 1996. Significance of interstitial coesite in eclogites from Yankou, Qingdao city, eastern China. Chin. Sci. Bull. 41, 1047–1048 (in Chinese).

Ye, K., Ye, D.N., Cong, B.L., 2000. The possible subduction of continental material to depths greater than 200 km. Nature 407, 734–736.

Zhai, M.G., Cong, B.L., Guo, J.H., Liu, W.J., Li, Y.G., Wang, Q.C., 2000. Division of petrological–tectonic units in the northern Sulu ultrahigh-pressure zone: An example of thick-skin thrust of crystalline units. Sci. Geol. Sin. 35, 16–26 (in Chinese with English abstract).

Zheng, Y.F., Wang, Z.R., Li, S.G., Zhao, Z.F., 2002. Oxygen isotope equilibrium between eclogite minerals and its constraints on mineral Sm–Nd chronometer. Geochim. Cosmochim. Acta 66, 625–634.

Zheng, Y.F., Fu, B., Gong, B., Li, H., 2003. Stable isotope geochemistry of ultrahigh pressure metamorphic rocks from the Dabie–Sulu orogen in China: implications for geodynamics and fluid regime. Earth Sci. Rev. 62, 105–161.

Zhi, X.C., Chen, D.G., Zhang, Z.Q., Wang, J.H., 1994. The neodymium and strontium isotopic compositions of Cenozoic alkali basalts from Penglai and Linqu, Shandong province. Geol. Rev. 40, 526–533 (in Chinese with English abstract).